ARS MATHEMATICA CONTEMPORANEA

Also available at http://amc-journal.eu
ISSN 1855-3966 (printed edn.), ISSN 1855-3974 (electronic edn.)
ARS MATHEMATICA CONTEMPORANEA 12 (2017) 315–327

A chiral 4-polytope in $\mathbb{R}^3$

Daniel Pellicer
Centro de Ciencias Matemáticas, UNAM, Campus Morelia
C.P. 58190, Morelia, Michoacán, México

Received 8 March 2016, accepted 29 August 2016, published online 21 January 2017

Abstract

In this paper we describe an infinite chiral 4-polytope in the Euclidean 3-space. This builds on previous work of Bracho, Hubard and the author, where a finite chiral 4-polytope in the Euclidean 4-space is constructed. These two polytopes show that there are finite and infinite chiral polytopes of full rank as defined by McMullen.

Keywords: Chiral 4-polytope, full rank polytope.

Math. Subj. Class.: 52B11

1 Introduction

In this paper we regard n-polytopes as combinatorial structures in $\mathbb{R}^d$ constructed from $(n-1)$-polytopes as building blocks, where 0- and 1-polytopes are points and line segments, respectively.

Regular polytopes are those admitting the highest degree of symmetry in the sense that any two flags are equivalent under the symmetry group. In some way they admit all possible abstract reflections as symmetries.

Nowadays we have plenty of examples of regular polytopes, the most obvious being the convex regular polytopes (see for example [2]) and the tessellations by n-dimensional cubes. Other examples of regular polytopes can be found in [4, 5, 6, 7].

Chiral polytopes have two orbits of flags under the symmetry group with the property that adjacent flags belong to distinct orbits. They admit all abstract rotations as symmetries, but no abstract reflection.

There is very little published work on chiral polytopes on Euclidean spaces. There are no convex chiral polytopes and no chiral tessellations of Euclidean spaces. This illustrates the difficulty to find 'natural' families of chiral polytopes.

In 2005 Schulte classified all chiral polyhedra in $\mathbb{R}^3$ (see [11] and [12]). They are all infinite; some have finite faces, and some have infinite faces.

E-mail address: pellicer@matmor.unam.mx (Daniel Pellicer)

In [5, Theorem 11.2] it was claimed that for any positive integer d there are neither finite chiral d-polytopes in $\mathbb{R}^d$, nor infinite chiral $(d+1)$-polytopes in $\mathbb{R}^d$.

The first known finite chiral 4-polytope in $\mathbb{R}^4$ was discovered in [1] in 2014 proving false one half of the claim in [5]. In this paper we describe the first known infinite chiral 4-polytope in $\mathbb{R}^3$, proving false the remaining half of the claim.

Definitions and basic results are given in Section 2. In Section 3 we describe the building blocks of the 4-polytope, which is constructed in Section 4. Finally, in Section 5 we discuss the combinatorial symmetry of the 4-polytope.

2 Preliminaries

In this section we recall some concepts and results of the Euclidean space and of polytopes embedded on it.

2.1 Symmetries of the Euclidean space

The rotation group of the octahedron, that we shall denote by $[3,4]^+$, is one of the finite groups of isometries of $\mathbb{R}^3$. It contains 24 elements, out of which six are 4-fold rotations, eight are 3-fold rotations, nine are half-turns, and the remaining one is the identity. In particular, all of its elements preserve orientation (see for example [3] for a more detailed description of this group).

A *lattice* is the orbit of the origin o under a discrete translation group of $\mathbb{R}^3$ generated by translations with respect to three linearly independent vectors. Up to similarity, there are three lattices that are invariant under the action of the group $[3,4]^+$ (see [8, Section 6D]).

The *cubic lattice*, denoted by $\Lambda_{(1,0,0)}$, consists of the points of $\mathbb{R}^3$ with integer coordinates. The translations by the vectors $(1,0,0)$, $(0,1,0)$ and $(0,0,1)$ constitute a basis for the translation group of this lattice.

The *face-centred cubic lattice*, denoted by $\Lambda_{(1,1,0)}$, is generated by the translations by the vectors $(1,1,0)$, $(1,0,1)$ and $(0,1,1)$. It contains the set of points of $\mathbb{R}^3$ with integer coordinates, whose sum is an even number. The cubic lattice is the union

$$\Lambda_{(1,1,0)} \cup (\Lambda_{(1,1,0)} + (1,0,0))$$

of two isometric copies of the face-centred cubic lattice.

Finally, the *body centred cubic lattice* is the set of points with integer coordinates such that either all of them are even, or all of them are odd. It is generated by the translations by the vectors $(1,1,1)$, $(-1,1,1)$ and $(1,-1,1)$, and it is denoted by $\Lambda_{(1,1,1)}$. The cubic lattice is the union

$$\Lambda_{(1,1,0)} \cup (\Lambda_{(1,1,0)} + (1,0,0)) \cup (\Lambda_{(1,1,0)} + (0,1,0)) \cup (\Lambda_{(1,1,0)} + (0,0,1))$$

of four isometric copies of the body-centred cubic lattice.

The tessellation $\{4,3,4\}$ by cubes of $\mathbb{R}^3$ is the only regular tessellation of the Euclidean space. A *Petrie polygon* of $\{4,3,4\}$ is a helix with vertex and edge sets contained in those of $\{4,3,4\}$, where every two consecutive edges belong to some square; every three consecutive edges belong to the same cube, but not to the same square; and no four consecutive edges belong to the same cube. The direction vectors of any three consecutive edges of a Petrie polygons of $\{4,3,4\}$ are precisely $(1,0,0)$,$(0,1,0)$ and $(0,0,1)$ in some order. These helices have axes with direction vectors $(1,1,1)$, $(1,1,-1)$, $(1,-1,1)$ and

$(-1, 1, 1)$. Every edge of a Petrie polygon h is a translate of any edge that is $3k$ steps apart in h (that is, there are $3k - 1$ edges between them).

Any two Petrie polygons of $\{4, 3, 4\}$ are isometric. However, any given Petrie polygon is equivalent under orientation preserving isometries (translations, rotations and twists) to only half of the Petrie polygons. We say that a Petrie polygon is a *right helix* if it can be obtained from the helix

$$\ldots, (1, 0, 0), (0, 0, 0), (0, 1, 0), (0, 1, 1), (-1, 1, 1), \ldots$$

by an orientation preserving isometry. The remaining helices are called *left helices*.

2.2 Polyhedra and 4-polytopes

When studying highly symmetric polytopes we need to move away from convexity to get a richer theory. The definitions below follow the spirit of [4] and subsequent papers.

For us a *polygon* (or 2-*polytope*) in $\mathbb{R}^3$ is a discrete set of points called *vertices* or *0-faces* together with a set of line segments called *edges* or *1-faces* between pairs of vertices, such that the resulting graph is connected and 2-regular. The edges are allowed to intersect in interior points, but there are no vertices in the interior of edges.

A *polyhedron* (or 3-*polytope*) in $\mathbb{R}^3$ is a set of polygons, called 2-*faces*, with the extra properties that every edge belongs to exactly two polygons, the set of vertices is discrete, the graph determined by the vertices and edges is connected, and the vertex-figures at all vertices are connected. Here the *vertex-figure* at a vertex v is the polygon (or in principle polygons) whose vertices are the neighbours of v, two of which are adjacent if and only if they are the two neighbours of v in a 2-face.

A 4-*polytope* in $\mathbb{R}^3$ is a set of polyhedra, called 3-*faces* with the extra properties that every 2-face belongs to exactly two polyhedra, the set of vertices is discrete, the graph determined by the vertices and edges is connected, and the vertex-figures at all vertices are polyhedra. The *vertex-figure* at a vertex v in this case consists of the polygons that are the vertex-figures at v in the polyhedra containing it.

Defined as above, polyhedra and 4-polytopes in $\mathbb{R}^3$ are precisely Euclidean realisations of abstract polyhedra and 4-polytopes as defined in [8, Section 5]. Due to this relationship, we say that two elements of an n-polytope are *incident* if one is contained in the other as geometric objects. Vertices, edges, polygons and polyhedra are then regarded as objects of rank 0, 1, 2 and 3, respectively.

The *facets* of an n-polytope are its $(n-1)$-faces ($n \in \{3, 4\}$). The 1-*skeleton* of a polyhedron or of a 4-poltyope is the graph determined by its sets of vertices and edges. The 2-*skeleton* of a 4-polytope consists of the sets of vertices, edges and 2-faces.

A *flag* of an n-polytope $\mathcal{P}$ is a set of n mutually incident elements of $\mathcal{P}$, one of each rank. That is, a flag of a polygon is a pair of incident vertex and edge, a flag of a polyhedron is a triple of mutually incident vertex, edge and 2-face, and a flag of a 4-polytope contains a vertex, an edge, a polygon and a polyhedron, all incident to the other three.

Given any flag Φ of an n-polytope and given $i \in \{0, \ldots, n-1\}$ there exists a unique flag Φ^i that differs from Φ only on the face of rank i. The flag Φ^i is known as the i-*adjacent* flag of Φ. We extend recursively this notion and for any word w on the elements in $\{0, \ldots, n-1\}$ we define $\Phi^{wi} := (\Phi^w)^i$.

By a *symmetry* of an n-polytope $\mathcal{P}$ we mean an isometry of $\mathbb{R}^3$ that preserves $\mathcal{P}$. An n-polytope is said to be *regular* whenever its symmetry group acts transitively on the flags

of $\mathcal{P}$. Clearly, the facets of a regular 4-polytope are regular polyhedra. There are 48 regular polyhedra and 8 regular 4-polytopes in $\mathbb{R}^3$; they were thoroughly studied in [7].

An n-polytope is said to be *chiral* whenever its symmetry group induces two orbits on the flags, with adjacent flags in distinct orbits. The term 'chiral' often carries the meaning of being handed, that is, not admitting a mirror symmetry. In our context, where only highly symmetric objects are of interest, chiral polytopes denote the most symmetric polytopes that do not admit a symmetry mapping a flag to an adjacent flag, which is the combinatorial equivalent to mirror symmetry.

There are no finite chiral polyhedra in $\mathbb{R}^3$ (see for example [11, Theorem 3.1]). Infinite chiral polyhedra were classified in [11] and [12] in six families. One of this polyhedra is described in detail in Section 3.

Regular and chiral n-polytopes admit a set of *distinguished abstract rotations* as symmetries. These are isometries S_i that map a given base flag Φ to the flag $\Phi^{i(i-1)}$ for $i \in \{1, \dots, n-1\}$. Such an isometry needs not be a rotation around an axis in $\mathbb{R}^3$. However, the term 'rotation' is in no way inadequate, since their combinatorial impact is similar to that of a rotation on a polygon. S_1 cyclically permutes the vertices and edges of the base 2-face, S_2 cyclically permutes the edges and polygons around the base vertex contained in the base polyhedron, and S_3 cyclically permutes the polygons and polyhedra around the base edge.

The symmetry group of a chiral n-polytope is generated by its distinguished abstract rotations. The group generated by all distinguished abstract rotations of a regular n-polytope has index at most 2 in the full symmetry group. The tetrahedron $\{3,3\}$ and its Petrial $\{4,3\}_3$ are examples of polyhedra where the subgroups generated by the distinguished abstract rotations have index 2 and 1, respectively.

Conversely, an n-polytope whose symmetry group contains all possible distinguished abstract rotations is either regular or chiral, and it is regular if and only if the symmetry group contains an element moving the base vertex but fixing all other elements of the base flag (see [13] for the combinatorial analogue to these claims).

3 The polyhedron $P_1(1,0)$

It is time now to describe the chiral polyhedron $P_1(1,0)$ as a particular case of the general description of the polyhedra $P_1(a,b)$ in [9]. Other description, using the technique known as Wythoff's construction, can be found in [12].

Throughout, $\mathcal{T}$ will denote the cubical tessellation $\{4,3,4\}$ of $\mathbb{R}^3$ with vertices on $\mathbb{Z}^3$, and $\eta : \mathbb{R}^3 \to \Pi$ the orthogonal projection into the plane Π through the origin o with normal vector $(1,1,1)$. It is well known that the image under η of the 1-skeleton of $\mathcal{T}$ is the 1-skeleton of a tessellation $\mathcal{T}'$ by equilateral triangles, and that $\Lambda_{(1,1,1)}\eta$ is the vertex set of a tessellation by equilateral trangles whose edge length is twice as that of $\mathbb{Z}^3\eta$. The preimage under η of any edge of $\mathcal{T}'$ intersects $\mathcal{T}$ in a collection of parallel edges.

Figure 1 shows the tessellation $\mathcal{T}'$ of Π on pale gray and black lines. Assume that the origin o projects to the fat vertex and that the coordinate axes project as indicated. That is, assume that one endpoint of the edge to the left of the fat vertex is the projection of $(1,0,0)$, that the black edge at the fat vertex that does not belong to the dotted path ends at the projection of $(0,0,1)$, and that one endpoint of the remaining black edge incident to the fat vertex is the projection of $(0,1,0)$.

Under these assumptions the polyhedron $P_1(1,0)$ can be described as follows. Its ver-

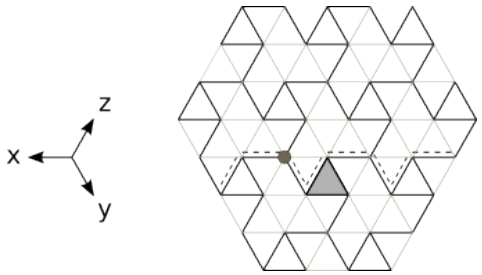

Figure 1: Projection of the 1-skeleton of $P_1(1,0)$

tex set is $\mathbb{Z}^3$. The edge set of $P_1(a,b)$ consists of all edges e of $\mathcal{T}$ such that $e\eta$ is a black edge in Figure 1, that is,

- the edge between (x,y,z) and $(x+1,y,z)$ for every $(x,y,z) \in \Lambda_{(1,1,1)}$ and $(x,y,z) \in \Lambda_{(1,1,1)} + (0,0,1)$,
- the edge between (x,y,z) and $(x,y+1,z)$ for every $(x,y,z) \in \Lambda_{(1,1,1)}$ and $(x,y,z) \in \Lambda_{(1,1,1)} + (1,0,0)$,
- the edge between (x,y,z) and $(x,y,z+1)$ for every $(x,y,z) \in \Lambda_{(1,1,1)}$ and $(x,y,z) \in \Lambda_{(1,1,1)} + (0,1,0)$.

Finally, the 2-faces are all Petrie polygons of $\mathcal{T}$ living in this 1-skeleton.

The six edges incident to any given vertex of $\mathcal{T}$ project by η to three gray edges and three black edges. This can be used to show that all vertices of $P_1(a,b)$ have degree 3. Since no two black edges at the same vertex in Figure 1 are collinear, the set of three edges incident to a vertex of $P_1(a,b)$ are translates of the three edges incident to some vertex of the cube $\mathcal{C}$ with vertex set $\{(x,y,z) : x,y,z, \in \{0,1\}\}$. The precise arrangement of edges at each vertex is explained by the following straightforward lemma.

Lemma 3.1. *The three edges incident to any vertex of $P_1(1,0)$ in $\Lambda_{(1,1,1)}$ are translates of the three edges incident to $(0,0,0)$ in the cube $\mathcal{C}$ defined as above. Similarly, the three edges incident to any vertex of $P_1(1,0)$ in $\Lambda_{(1,1,1)} + (1,0,0)$ (resp. in $\Lambda_{(1,1,1)} + (0,1,0)$ and $\Lambda_{(1,1,1)} + (0,0,1)$) are translates of the three edges of $\mathcal{C}$ incident to $(1,0,1)$ (resp. to $(1,1,0)$ and to $(0,1,1)$).*

The 2-faces of $P_1(1,0)$ are helices over triangles and belong to four parallel classes $\mathcal{H}_1, \mathcal{H}_2, \mathcal{H}_3, \mathcal{H}_4$. Helices in $\mathcal{H}_1$ project to the triangles with black edges in Figure 1. Every helix in $\mathcal{H}_2$ projects to Π either in the path with dashed lines or in one of its translates. Helices in $\mathcal{H}_3$ and $\mathcal{H}_4$ project to images of helices in $\mathcal{H}_2$ under rotations by $2\pi/3$ and by $4\pi/3$, respectively.

The axis of every helix in $\mathcal{H}_1$ has direction vector $(1,1,1)$. There is precisely one helix in $\mathcal{H}_1$ projecting to each triangle in Figure 1. For example, the helix

$$\ldots, (-1,0,-1), (-1,0,0), (-1,1,0), (0,1,0), (0,1,1), (0,2,1), \ldots \tag{3.1}$$

is the only helix that projects to the triangle with gray interior. All other helices in $\mathcal{H}_1$ are obtained by translating this helix by integer combinations of $(1,1,-1)$ and $(1,-1,1)$.

In contrast, infinitely many helices in $\mathcal{H}_2$ project to the dotted path. They are the helix

$$\ldots,(1,-1,-1),(1,0,-1),(1,0,0),(0,0,0),(0,1,0),(0,1,1),(-1,1,1),\ldots \tag{3.2}$$

and its translates by $m(1,1,1)$ for $m \in \mathbb{Z}$. The remaining helices in $\mathcal{H}_2$ are obtained by translating these helices by $m(1,1,-1)$ for $m \in \mathbb{Z}$. They all have direction vector $(-1,1,1)$.

The parallel classes $\mathcal{H}_3$ and $\mathcal{H}_4$ are respectively represented by the helices

$$\ldots,(-1,1,-1),(-1,1,0),(0,1,0),(0,0,0),(0,0,1),(1,0,1),(1,-1,1),\ldots, \tag{3.3}$$

$$\ldots,(-1,-1,1),(0,-1,1),(0,0,1),(0,0,0),(1,0,0),(1,1,0),(1,1,-1),\ldots, \tag{3.4}$$

which have the same projection to Π as their translates by $m(1,1,1)$ with $m \in \mathbb{Z}$. All other helices in each of these classes are obtained by translating these helices by $m(-1,1,1)$ for $m \in \mathbb{Z}$. The axis of every helix in $\mathcal{H}_3$ (resp. $\mathcal{H}_4$) has direction vector $(1,-1,1)$ (resp. $(1,1,-1)$).

It should be clear now that every edge in a black-edged triangle in Figure 1 is in the projection of a helix in $\mathcal{H}_1$ and of a helix in some other parallel class. The horizontal edges in black-edged triangles are the projection of helices in $\mathcal{H}_1$ and $\mathcal{H}_3$; those edges in black-edged triangles that are translates of the edge in the gray triangle that belongs also to the dotted path are projections of helices in $\mathcal{H}_1$ and $\mathcal{H}_2$; and the remaining edges in black-edged triangles are projections of helices in $\mathcal{H}_1$ and $\mathcal{H}_4$. Similarly, every black edge in Figure 1 that is not in a triangle belongs to the projection of helices in precisely two of the parallel classes $\mathcal{H}_2$, $\mathcal{H}_3$ and $\mathcal{H}_4$. From this it is easy to see that every edge of $P_1(1,0)$ belongs precisely to two helices. Furthermore, the parallel classes of the helices containing an edge e are completely determined by whether or not $e\eta$ belongs to a black-edged triangle, together with its direction vector in Figure 1.

In order to discuss the symmetries of $P_1(1,0)$ we take as base flag Φ the one containing the origin o, the edge between o and $(0,1,0)$, and the helix in (3.2). Let S_1 be the screw motion

$$(x,y,z) \mapsto (-y+1,z,-x) \tag{3.5}$$

with axis $\left\{\frac{1}{3}(1,1,0)+k(-1,1,1) \,:\, k \in \mathbb{R}\right\}$, translation vector $\frac{1}{3}(1,-1,-1)$ and rotation component of $2\pi/3$. Let S_2 be the rotation

$$(x,y,z) \mapsto (z,x,y) \tag{3.6}$$

about the axis $\{k(1,1,1) \,:\, k \in \mathbb{R}\}$ by an angle of $2\pi/3$. By applying these isometries to the edges of $P_1(1,0)$ we can see that S_1 and S_2 preserve the 1-skeleton of $P_1(1,0)$. Hence, S_1 and S_2 also preserve the set of 2-faces of $P_1(a,b)$. Furthermore, S_1 cyclically permutes the vertices of the base 2-face and S_2 cyclically permutes the three helices around o. This implies that $P_1(1,0)$ admits symmetries acting like the distinguished abstract rotations and therefore it is either regular or chiral.

The polyhedron $P_1(1,0)$ turns out to be chiral. Indeed, the only isometry T preserving the base edge and base helix, but interchanging the base vertex o with $(0,1,0)$ is the half-turn

$$(x,y,z) \mapsto (z,-y+1,x)$$

with axis $\{(0,1/2,0)+k(1,0,1) \,:\, k \in \mathbb{R}\}$. However, such a T maps the edge between o and $(0,0,1)$ to the edge between $(0,1,0)$ and $(1,1,0)$, which is not an edge of $P_1(1,0)$, and hence does not preserve the 1-skeleton of $P_1(1,0)$.

The base helix of $P_1(1,0)$ is a right helix as explained in Section 2. The symmetries S_1 and S_2 defined above are both orientation preserving. It follows that all helices in $P_1(1,0)$ are right helices.

The symmetry S_1^3 of $P_1(1,0)$ is the translation by the vector $(1,-1,-1)$. The conjugates of this translation by S_2 and S_2^2 are the translations by the vectors $(-1,1,-1)$ and $(-1,-1,1)$, respectively. The next proposition follows.

Proposition 3.2. *The symmetry group of $P_1(1,0)$ contains the translations by all vectors with endpoints in $\Lambda_{(1,1,1)}$.*

Since $P_1(1,0)$ is chiral, it is also helix-transitive, implying the next remark.

Remark 3.3. The orthogonal projections of $P_1(1,0)$ in the directions $(1,1,-1)$, $(1,-1,1)$ and $(-1,1,1)$ of the axes of the helices are all isometric to the projection in the direction $(1,1,1)$ in Figure 1.

It is interesting to note that the set of gray edges in Figure 1 is isometric to the set of black edges, and one can be obtained from the other by a half-turn around the fat point. The polyhedron constructed from the preimages in $\mathcal{T}$ of the gray edges under the projection η is clearly isometric to $P_1(1,0)$ but it contains only left helices. They are precisely the images of the helices of $P_1(1,0)$ under the isometry mapping $\bar{x}$ to $-\bar{x}$ for every $\bar{x} \in \mathbb{R}^3$.

4 The chiral 4-polytope $\mathcal{P}_{\{\infty,3,4\}}$

The polyhedron $P_1(1,0)$ just described is the building block of the chiral 4-polytope $\mathcal{P}_{\{\infty,3,4\}}$. The vertex and edge sets of $\mathcal{P}_{\{\infty,3,4\}}$ are the vertex and edge sets of the cubic tessellation $\mathcal{T}$. The 2-faces of $\mathcal{P}_{\{\infty,3,4\}}$ are all right Petrie polygons of $\mathcal{T}$. This set constitutes the regular polygonal complex $\mathcal{K}_7(1,1)$ in [10].

The facets of $\mathcal{P}_{\{\infty,3,4\}}$ are $P_1(1,0)$ and its images under the group $[3,4]^+$ of rotations of the octahedron. Recall that $[3,4]^+$ has 24 elements. Since $P_1(1,0)$ is invariant under three-fold rotations around the line through o with direction vector $(1,1,1)$, there are at most 8 images of $P_1(1,0)$ under $[3,4]^+$.

In fact, $\mathcal{P}_{\{\infty,3,4\}}$ has precisely 8 facets. They are described next. Recall from Section 3 that the three neighbours of o in $P_1(1,0)$ are $e_1 = (1,0,0)$, $e_2 = (0,1,0)$ and $e_3 = (0,0,1)$. This motivates to denote this polyhedron as a facet of $\mathcal{P}_{\{\infty,3,4\}}$ by $F_{(+,+,+)}$. The group $[3,4]^+$ acts transitively on the set of octants of $\mathbb{R}^3$ and hence $\mathcal{P}_{\{\infty,3,4\}}$ has precisely 8 facets. They are denoted $F_{(a_1,a_2,a_3)}$, where a_i takes the value '+' whenever in that facet e_i is a neighbour of o, and the value '$-$' otherwise. For example, the orbit of $F_{(+,+,+)}$ under the 4-fold rotation around the z axis mapping (x,y,z) to $(y,-x,z)$ is

$$(F_{(+,+,+)}, F_{(+,-,+)}, F_{(-,-,+)}, F_{(-,+,+)}).$$

In order to better understand the combinatorics of $\mathcal{P}_{\{\infty,3,4\}}$ it is convenient to compute the image of all its facets under the projection η as defined in Section 3. This can be done by directly applying the orientation preserving isometries in $[3,4]^+$ and then η to the edges of $P_1(1,0)$.

Alternatively, we can use the fact that the helices of $P_1(1,0)$ split in four classes $\mathcal{H}_1$, $\mathcal{H}_2$, $\mathcal{H}_3$ and $\mathcal{H}_4$, consisting of helices with axes having direction vector $(1,1,1)$, $(-1,1,1)$, $(1,-1,1)$ and $(1,1,-1)$, respectively. Every isometry $T \in [3,4]^+$ permutes the four directions $(1,1,1)$, $(1,1,-1)$, $(1,-1,1)$ and $(-1,1,1)$ of the axes of helices of $P_1(1,0)$ and

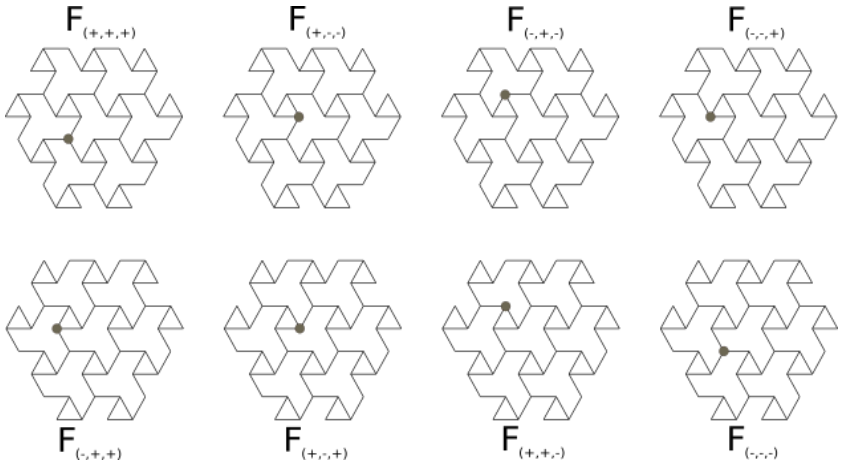

Figure 2: Projections of the eight facets of $\mathcal{P}_{\{\infty,3,4\}}$

so $F_{(+,+,+)}T$ must have a parallel class of helices with axes in the direction of $(1,1,1)$. These helices project orthogonally into triangles on the plane Π; furthermore, this triangles must be pointing up, since they are precisely the images of right helices, whereas the left helices project into triangles pointing down. Similarly, the helices in the three remaining parallel classes must project into isometric copies of the dotted path in Figure 1. This information, together with the three neighbours of o on each facet and Remark 3.3, determines the projections of the eight facets of $\mathcal{P}_{\{\infty,3,4\}}$ as in Figure 2, where the fat dot represents the origin o.

We can see that $F_{(+,+,+)}$ and $F_{(-,-,-)}$ are the only facets where o does not belong to a helix with axis in the direction of $(1,1,1)$. In both instances o belongs to helices with axes in the directions of $(-1,1,1)$, $(1,-1,1)$ and $(1,1,-1)$.

We choose the following seven isometries $T_{(a_1,a_2,a_3)} \in [3,4]^+$ mapping $F_{(+,+,+)}$ to $F_{(a_1,a_2,a_3)}$:

$$\begin{aligned}
T_{(+,-,-)} &: (x,y,z) \mapsto (x,-y,-z),\\
T_{(-,+,-)} &: (x,y,z) \mapsto (-x,y,-z),\\
T_{(-,-,+)} &: (x,y,z) \mapsto (-x,-y,z),\\
T_{(-,+,+)} &: (x,y,z) \mapsto (-z,y,x),\\
T_{(+,-,+)} &: (x,y,z) \mapsto (y,-x,z),\\
T_{(+,+,-)} &: (x,y,z) \mapsto (x,z,-y),\\
T_{(-,-,-)} &: (x,y,z) \mapsto (-x,-y,-z).
\end{aligned}$$

We also denote by H_1, H_2, H_3 and H_4 the helices in (3.1), (3.2), (3.3) and (3.4), respectively. Recall that the helices in $F_{(+,+,+)}$ with direction vector $(1,1,1)$ are H_1 and its translates by vectors with endpoints in $\Lambda_{(1,1,1)}$.

The right Petrie polygons of $\mathcal{T}$ with axes in the direction of $(1,1,1)$ are the ones in $F_{(+,+,+)}$ together with their translates by $(1,0,0)$, $(0,1,0)$ and $(0,0,1)$. It can be seen from Figure 2 that the helices in $F_{(+,+,+)}$ with axis in the direction of $(1,1,1)$ are also

helices of $F_{(-,-,-)}$. Furthermore, the helices with axes in the direction of $(1,1,1)$ of $F_{(+,-,-)}$ and of $F_{(+,-,+)}$ are the translates of those in $F_{(+,+,+)}$ by $(0,0,1)$, the helices with axes in the direction of $(1,1,1)$ of $F_{(-,+,-)}$ and of $F_{(+,+,-)}$ are the translates of those in $F_{(+,+,+)}$ by $(1,0,0)$, and the helices with axes in the direction of $(1,1,1)$ of $F_{(-,-,+)}$ and of $F_{(-,+,+)}$ are the translates of those in $F_{(+,+,+)}$ by $(0,1,0)$. This can also be verified by noting that

$$\begin{aligned} H_1 &= H_1T_{(-,-,-)} + (-1,1,1), \\ H_1 + (1,-1,1) &= H_2T_{(+,-,-)} + (0,0,1) = H_2T_{(+,-,+)} + (0,0,1), \\ H_1 + (1,-1,-1) &= H_3T_{(-,+,-)} + (1,0,0) = H_3T_{(+,+,-)} + (1,0,0), \\ H_1 &= H_4T_{(-,-,+)} + (0,1,0) = H_4T_{(-,+,+)} + (0,1,0), \end{aligned}$$

together with the fact that $[3,4]^+$ permutes the four directions of the axes of the helices of $F_{(+,+,+)}$ and that the set of helices of $F_{(+,+,+)}$ in any of the four directions is invariant by translations by vectors with endpoints in $\Lambda_{(1,1,1)}$. This shows that all right Petrie polygons of $\mathcal{T}$ with axes in the direction of $(1,1,1)$ belong to at least two facets of $\mathcal{P}_{\{\infty,3,4\}}$. Recall that the set of helices on $P_1(1,0)$ with axis in the direction of $(1,1,1)$ can be obtained by translating H_1 by vectors with endpoints in $\Lambda_{(1,1,1)}$, and similarly the set of helices of $P_1(1,0)$ with axis in the direction of $(-1,1,1)$, $(1,-1,1)$ or $(1,1,-1)$ can be obtained by translating H_2, H_3 or H_4, respectively, by vectors with endpoints in $\Lambda_{(1,1,1)}$. This shows that each right Petrie polygon of $\mathcal{T}$ with axis in the direction of $(1,1,1)$ belongs to precesely two facets of $\mathcal{P}_{\{\infty,3,4\}}$. The fact that $\mathcal{T}$ and $\mathcal{P}_{\{\infty,3,4\}}$ are symmetric under $[3,4]^+$ implies the following lemma.

Lemma 4.1. *Every helix of $\mathcal{P}_{\{\infty,3,4\}}$ belongs to precisely two facets.*

Table 1 indicates the direction vector of the helices that two facets have in common (if any). In the table, (a_1,a_2,a_3) indicates the facet $F_{(a_1,a_2,a_3)}$. In particular one can conclude that the facets $F_{(a_1,a_2,a_3)}$ and $F_{(b_1,b_2,b_3)}$ have a helix in common if (a_1,a_2,a_3) and (b_1,b_2,b_3) coincide either in two coordinates or in none. The entries on the table can be obtained by applying the isometries $T_{(a_1,a_2,a_3)}$ to the helices of $F_{(+,+,+)}$, or by a careful inspection of Figure 2.

Facets	$(+,+,+)$	$(+,+,-)$	$(+,-,+)$	$(-,+,+)$	$(+,-,-)$	$(-,+,-)$	$(-,-,+)$	$(-,-,-)$
$(+,+,+)$	—	$(-1,1,1)$	$(1,1,-1)$	$(1,-1,1)$	none	none	none	$(1,1,1)$
$(+,+,-)$	$(-1,1,1)$	—	none	none	$(1,-1,1)$	$(1,1,1)$	$(1,1,-1)$	none
$(+,-,+)$	$(1,1,-1)$	none	—	none	$(1,1,1)$	$(1,-1,1)$	$(-1,1,1)$	none
$(-,+,+)$	$(1,-1,1)$	none	none	—	$(-1,1,1)$	$(1,1,-1)$	$(1,1,1)$	none
$(+,-,-)$	none	$(1,-1,1)$	$(1,1,1)$	$(-1,1,1)$	—	none	none	$(1,1,-1)$
$(-,+,-)$	none	$(1,1,1)$	$(1,-1,1)$	$(1,1,-1)$	none	—	none	$(-1,1,1)$
$(-,-,+)$	none	$(1,1,-1)$	$(-1,1,1)$	$(1,1,1)$	none	none	—	$(1,-1,1)$
$(-,-,-)$	$(1,1,1)$	none	none	none	$(1,1,-1)$	$(-1,1,1)$	$(1,-1,1)$	—

Table 1: Helices shared by two facets of $\mathcal{P}_{\{\infty,3,4\}}$.

Recall that the vertex-figure at o in $\mathcal{P}_{\{\infty,3,4\}}$ consists of the eight triangles that are the vertex-figures at o of the eight facets of $\mathcal{P}_{\{\infty,3,4\}}$. From the construction it is immediate that the vertex-figure at o in $\mathcal{P}_{\{\infty,3,4\}}$ is an octahedron.

As a consequence of Proposition 3.2, the three neighbours in $F_{(+,+,+)}$ of any vertex v in $\Lambda_{(1,1,1)}$ are $v+(1,0,0)$, $v+(0,1,0)$ and $v+(0,0,1)$. A similar statement can be made for the remaining seven facets of $\mathcal{P}_{\{\infty,3,4\}}$. Indeed, since $F_{(a_1,a_2,a_3)}$ is the image of $F_{(+,+,+)}$ under some isometry in $[3,4]^+$ and $\Lambda_{(1,1,1)}$ is invariant under the entire group $[3,4]^+$, the translations by vectors with endpoints in $\Lambda_{(1,1,1)}$ are symmetries of $F(a_1,a_2,a_3)$. This implies that the vertex-figure at any vertex of $\mathcal{P}_{\{\infty,3,4\}}$ in $\Lambda_{(1,1,1)}$ is an octahedron. This statement is in fact true for any vertex of $\mathcal{P}_{\{\infty,3,4\}}$.

Lemma 4.2. *The vertex-figure of any vertex of $\mathcal{P}_{\{\infty,3,4\}}$ is an octahedron.*

Proof. Since every facet of $\mathcal{P}_{\{\infty,3,4\}}$ is invariant under translations by vectors with endpoints in $\Lambda_{(1,1,1)}$, we only need to show that the result holds for a representative of each translation class. Since $\Lambda_{(1,0,0)}$ is the disjoint union of four translates of $\Lambda_{(1,1,1)}$, there are only four orbits of vertices of $\mathcal{P}_{\{\infty,3,4\}}$ under the action of the translations by vectors with endpoints in $\Lambda_{(1,1,1)}$. We take o, $(1,0,0)$, $(0,1,0)$ and $(0,0,1)$ as representatives of these orbits.

The previous discussion shows that the result holds for o (and hence for vertices in $\Lambda_{(1,1,1)}$). A close inspection to Figure 2 (or direct verification) shows that the neighbours of the remaining three representatives in facet $F_{(a_1,a_2,a_3)}$ are as in Table 2, where an entry (b_1,b_2,b_3) indicates that v has as neighbour $v+e_i$ when b_i is '+', and $v-e_i$ when b_i is '−'.

	$F_{(+,+,+)}$	$F_{(+,+,-)}$	$F_{(+,-,+)}$	$F_{(-,+,+)}$	$F_{(+,-,-)}$	$F_{(-,+,-)}$	$F_{(-,-,+)}$	$F_{(-,-,-)}$
$(1,0,0)$	$(-,+,-)$	$(-,-,-)$	$(-,+,+)$	$(+,-,+)$	$(-,-,+)$	$(+,+,+)$	$(+,-,-)$	$(+,+,-)$
$(0,1,0)$	$(-,-,+)$	$(+,-,+)$	$(+,+,-)$	$(-,-,-)$	$(-,+,-)$	$(+,-,-)$	$(+,+,+)$	$(-,+,+)$
$(0,0,1)$	$(+,-,-)$	$(-,+,+)$	$(-,-,-)$	$(+,+,-)$	$(+,+,+)$	$(-,-,+)$	$(-,+,-)$	$(+,-,+)$

Table 2: Neighbours of $(1,0,0)$, $(0,1,0)$ and $(0,0,1)$ on the facets of $\mathcal{P}_{\{\infty,3,4\}}$.

The entry of Table 2 corresponding to vertex v and facet F indicates the octant determined by the three neighbours of v in F. The vertex-figure of v at F is then a triangle in that octant (determined by the three neighbours of v). All octants appear exactly once on each row, implying that the vertex-figures are all octahedra. □

We are now ready for our main result.

Theorem 4.3. *The structure $\mathcal{P}_{\{\infty,3,4\}}$ is a chiral 4-polytope in $\mathbb{R}^3$.*

Proof. We know that $\mathcal{P}_{\{\infty,3,4\}}$ is the set of polyhedra

$$\{P_1(1,0)\alpha \,:\, \alpha \in [3,4]^+\},$$

and that the set of vertices is descrete. We also know that its 1-skeleton coincides with that of the tessellation by cubes, and hence it is connected. Every 2-face belongs to precisely two facets by Lemma 4.1 and all vertex-figures are polyhedra by Lemma 4.2. Hence $\mathcal{P}_{\{\infty,3,4\}}$ is a 4-polytope.

By construction, $\mathcal{P}_{\{\infty,3,4\}}$ is invariant under the rotation S_2 defined in (3.6) and the rotation S_3 given by

$$(x, y, z) \mapsto (z, y, -x),$$

since they just permute the images of $P_1(1, 0)$ under $[3, 4]^+$. Furthermore, the screw motion S_1 defined in (3.5) also preserves $\mathcal{P}_{\{\infty,3,4\}}$. In fact, by applying S_1 to the edge set of $F_{(a_1,a_2,a_3)}$ for each (a_1, a_2, a_3) we can see that S_1 fixes $F_{(+,+,+)}$ and $F_{(+,+,-)}$, and induces the permutation

$$\left(F_{(+,-,+)}, F_{(-,-,-)}, F_{(-,+,+)}\right) \cdot \left(F_{(+,-,-,)}, F_{(-,-,+)}, F_{(-,+,-)}\right)$$

in the remaining 6 facets of $\mathcal{P}_{\{\infty,3,4\}}$.

These three isometries are the distinguished abstract rotations with respect to the flag Ψ containing o, the edge between o and $(0, 1, 0)$, the helix in (3.2) and the facet $F_{(+,+,+)}$. Indeed, it is not hard to verify that $\Psi S_1 = \Psi^{10}$, $\Psi S_2 = \Psi^{21}$ and $\Psi S_3 = \Psi^{32}$. Hence $\mathcal{P}_{\{\infty,3,4\}}$ is either regular or chiral, and since its facets are chiral, $\mathcal{P}_{\{\infty,3,4\}}$ itself is chiral. □

5 Combinatorial symmetry

In the previous section we constructed a 4-polytope that is chiral as a geometric object. In this section we discuss its combinatorial nature. That is, we study $\mathcal{P}_{\{\infty,3,4\}}$ as a partially ordered set with a rank function ranging in $\{0, 1, 2, 3\}$, whose elements are the vertices, edges, polygons and polyhedra of $\mathcal{P}_{\{\infty,3,4\}}$ where two of them are incident if and only if one is contained in the other (see [8] for proper definitions of abstract polytopes).

An *automorphism* of an n-polytope is a bijection of its vertices, edges, etc. that preserves the incidence. A polytope is *combinatorially regular* (resp. *combinatorially chiral*) if its automorphism group acts transitively on its flags (resp. if its automorphism group induces two orbits on flags with adjacent flags in distinct orbits). The distinguished abstract rotations of $\mathcal{P}_{\{\infty,3,4\}}$ as a geometric object induce automorphisms as an abstract object.

Due to the connectivity of $\mathcal{P}_{\{\infty,3,4\}}$ and to the uniqueness of i-adjacent flags for $i \in \{0, 1, 2, 3\}$, any automorphism of $\mathcal{P}_{\{\infty,3,4\}}$ is completely determined by the image on any flag. As a consequence of this, the group generated by the automorphisms given by the abstract distinguished rotations of $\mathcal{P}_{\{\infty,3,4\}}$ has index at most 2 on the full automorphism group of $\mathcal{P}_{\{\infty,3,4\}}$. Furthermore, $\mathcal{P}_{\{\infty,3,4\}}$ is combinatorially regular if and only if there is an automorphism mapping a flag Φ to its 1-adjacent flag Φ^1. We next show that this is not the case.

Theorem 5.1. *The 4-polytope $\mathcal{P}_{\{\infty,3,4\}}$ is combinatorially chiral.*

Proof. We take as base flag $\Psi := \{F_0, F_1, F_2, F_3\}$ where $F_0 = o$, F_1 is the edge between o and $(0, 1, 0)$, F_2 is the helix in (3.2), and $F_3 = F_{(+,+,+)}$. We will show that $\mathcal{P}_{\{\infty,3,4\}}$ is abstractly chiral by assuming that there exists an automorphism R_1 mapping Ψ to Ψ^1, and showing that the image of the vertex $(1, -1, 1)$ under such R_1 is not well defined. In doing so we will abuse notation and use the geometric names and descriptions of the vertices, edges, 2-faces and facets, but the arguments to deduce the action of R_1 will be purely combinatorial (not geometric).

Since R_1 fixes F_2 and o while moving F_1, it must interchange the neighbours of o in F_2, namely $(1, 0, 0)$ and $(0, 1, 0)$. The facet F_3 also is fixed by R_1, and o belongs to three

edges in F_3. Since R_1 interchages the edge between o and $(1,0,0)$ with F_1, it must fix the remaining edge, that is, the edge between o and $(0,0,1)$; in particular $(0,0,1)R_1 = (0,0,1)$. This implies that the helices H_3 in (3.3) and H_4 in (3.4) are also interchanged by R_1, and so R_1 interchanges $(1,0,1)$ with $(0,-1,1)$ and $(1,-1,1)$ with $(-1,-1,1)$.

Now, since R_1 fixes F_3 but interchanges H_3 and H_4, it must also interchange the facets $F_{(-,+,+)}$ and $F_{(+,-,+)}$ since they are the only facets containing H_3 and H_4, respectively, other than $F_{(+,+,+)}$. The edge between o and $(0,0,1)$ is contained in precisely the four facets $F_{(+,+,+)}$, $F_{(-,+,+)}$, $F_{(+,-,+)}$ and $F_{(-,-,+)}$. The first of these facets is fixed by R_1 while the second and third are interchanged. Since R_1 fixes the edge between o and $(0,0,1)$, it must also fix the facet $F_{(-,-,+)}$.

Thus R_1 fixes $F_{(-,-,+)}$ and the edge between o and $(0,0,1)$. The remaining edges of $F_{(-,-,+)}$ containing o have their other endpoints in $(-1,0,0)$ and $(0,-1,0)$. The edge between o and $(-1,0,0)$ is also an edge of $F_{(-,+,+)}$ but not of $F_{(+,-,+)}$, whereas the edge between o and $(0,-1,0)$ is also an edge of $F_{(+,-,+)}$ but not of $F_{(-,+,+)}$. Therefore R_1 must interchange the edge between o and $(-1,0,0)$ with the edge between o and $(0,-1,0)$. In $F_{(-,-,+)}$ there is only one helix containing these two edges, and so it must be preserved by R_1. This helix is $H_2T_{(-,-,+)}$ with vertices

$$\ldots,(-1,1,-1),(-1,0,-1),(-1,0,0),(0,0,0),(0,-1,0),(0,-1,1),(1,-1,1),\ldots\ ,$$

and so R_1 must interchange $(0,-1,1)$ with $(-1,0,-1)$, and $(1,-1,1)$ with $(-1,1,-1)$. But we showed before that $(1,-1,1)R_1 = (-1,-1,1)$. This yields the desired contradiction. □

6 Acknowledgements

This work was supported by PAPIIT-UNAM under grant IN101615. The author thanks the anonymous referee for helpful suggestions.

References

[1] J. Bracho, I. Hubard and D. Pellicer, A finite chiral 4-polytope in $\mathbb{R}^4$, *Discrete Comput. Geom.* **52** (2014), 799–805, doi:10.1007/s00454-014-9631-4, http://dx.doi.org/10.1007/s00454-014-9631-4.

[2] H. S. M. Coxeter, *Regular polytopes*, Dover Publications, Inc., New York, 3rd edition, 1973.

[3] L. C. Grove and C. T. Benson, *Finite reflection groups*, volume 99 of *Graduate Texts in Mathematics*, Springer-Verlag, New York, 2nd edition, 1985, doi:10.1007/978-1-4757-1869-0, http://dx.doi.org/10.1007/978-1-4757-1869-0.

[4] B. Grünbaum, Regular polyhedra—old and new, *Aequationes Math.* **16** (1977), 1–20.

[5] P. McMullen, Regular polytopes of full rank, *Discrete Comput. Geom.* **32** (2004), 1–35, doi:10.1007/s00454-004-0848-5, http://dx.doi.org/10.1007/s00454-004-0848-5.

[6] P. McMullen, Regular polytopes of nearly full rank, *Discrete Comput. Geom.* **46** (2011), 660–703, doi:10.1007/s00454-011-9335-y, http://dx.doi.org/10.1007/s00454-011-9335-y.

[7] P. McMullen and E. Schulte, Regular polytopes in ordinary space, *Discrete Comput. Geom.* **17** (1997), 449–478, doi:10.1007/PL00009304, http://dx.doi.org/10.1007/PL00009304.

[8] P. McMullen and E. Schulte, *Abstract Regular Polytopes*, Cambridge University Press, 2002.

[9] D. Pellicer and A. Ivić Weiss, Combinatorial structure of Schulte's chiral polyhedra, *Discrete Comput. Geom.* **44** (2010), 167–194, doi:10.1007/s00454-010-9247-2, http://dx.doi.org/10.1007/s00454-010-9247-2.

[10] D. Pellicer and E. Schulte, Regular polygonal complexes in space, II, *Trans. Amer. Math. Soc.* **365** (2013), 2031–2061, doi:10.1090/S0002-9947-2012-05684-4, http://dx.doi.org/10.1090/S0002-9947-2012-05684-4.

[11] E. Schulte, Chiral polyhedra in ordinary space. I, *Discrete Comput. Geom.* **32** (2004), 55–99, doi:10.1007/s00454-004-0843-x, http://dx.doi.org/10.1007/s00454-004-0843-x.

[12] E. Schulte, Chiral polyhedra in ordinary space. II, *Discrete Comput. Geom.* **34** (2005), 181–229, doi:10.1007/s00454-005-1176-0, http://dx.doi.org/10.1007/s00454-005-1176-0.

[13] E. Schulte and A. I. Weiss, Chiral polytopes, in: *Applied geometry and discrete mathematics*, Amer. Math. Soc., Providence, RI, volume 4 of *DIMACS Ser. Discrete Math. Theoret. Comput. Sci.*, pp. 493–516, 1991.